CELL CYCLE
2020, VOL. 19, NO. 3, 339–353
https://doi.org/10.1080/15384101.2019.1711305

Taylor & Francis
Taylor & Francis Group

RESEARCH PAPER

Check for updates

Human umbilical cord mesenchymal stem cells-derived exosomes transfers microRNA-19a to protect cardiomyocytes from acute myocardial infarction by targeting SOX6

Lin Huang, Lu Yang, Yin Ding, Xinghua Jiang, Zhen Xia, and Zhigang You

Department of Cardiovascular Medicine, The Second Affiliated Hospital of Nanchang University, Nanchang, Jiangxi, P.R. China

ABSTRACT

Exosomes secreted by human umbilical cord mesenchymal stem cells (hucMSCs) protect cardiomyocytes from anoxia-reoxygenation injury. But the mechanism of hucMSC-exo-microRNA (miR)-19a in acute myocardial infarction (AMI) remains unclear. For this study, cardiac function related indicators, inflammatory factors and markers of myocardial injury, cardiomyocyte injury, infarct size, and apoptosis were detected *in vivo* experiments. The gain-and loss-of function was performed to evaluate the effects of hucMSC-exo with down/upregulated miR-19a on AMI rats and hypoxic H9C2 cells. Western blot analysis was used to detect levels of AKT/JNK3/caspase-3 axis-related proteins. Consequently, hucMSC-exo alleviated AMI and inhibited cardiomyocyte apoptosis. miR-19a was downregulated in AMI tissues and cells, and increased after hucMSC-exo treatment. miR-19a knockdown in hucMSC-exo impaired the protective role of hucMSC-exo alone in the AMI damage. SOX6 is a target gene of miR-19a and its inhibition lightened hypoxic damage of H9C2 cells. SOX6 knockdown together with miR-19a inhibition in hucMSC-exo activated AKT and inhibited JNK3/caspase-3 axis. Taken together, hucMSC-exo protected cardiomyocytes from AMI injury by transferring miR-19a, targeting SOX6, activating AKT, and inhibiting JNK3/caspase-3 activation. This study may provide new understanding for AMI treatment.

ARTICLE HISTORY
Received 25 September 2019
Revised 17 November 2019
Accepted 29 December 2019

KEYWORDS
Acute myocardial infarction; Human umbilical cord mesenchymal stem cells; Exosomes; microRNA-19a; SOX6; AKT/JNK3/caspase-3 axis

1. Introduction

Acute myocardial infarction (AMI) is caused by sudden coronary artery occlusion and myocardial necrosis, resulting from acute and persistent ischemia and hypoxia, which contributes to at least 500,000 new cases annually over the world [1,2]. AMI most often occurs when atherosclerotic plaques rupture into the coronary artery, which may lead to thrombosis and arterial obstruction, stopping the blood supply in the heart region, and leading to necrosis in the affected area [3]. Smoking is the most prevalent risk factor for AMI, followed by hypertension, family history of coronary artery disease, hyperlipidemia, vessel disease, metabolic syndrome, diabetes mellitus, insulin resistance, chest pain, angina and advancing age [4]. Additionally, AMI triggers an intense-inflammatory response, and accompanies with cardiomyocyte death, cardiac dysfunction and ventricular remodeling, probably endowing AMI patients high risk of heart failure, cardiogenic shock, ventricular fibrillation and recurrent ischemia [5,6]. Fortunately, evidence indicates that stem cell treatment is safe and moderately beneficial for regeneration of damaged vascular and cardiac tissue after AMI [3]. Enlightened by these, we aim to figure-out novel insights for AMI treatment from the aspect of human umbilical cord-derived MSCs (hucMSCs).

Studies have indicated mesenchymal stem cells (MSCs) are attractive in regenerative medicines due to their abilities of self-renewal, regeneration of damaged tissues and multilineage differentiation, and functions in regulating immunocompetent cell responses [7,8]. While hucMSCs get much attention in regeneration, and exert significant roles in alleviating liver fibrosis, promoting liver and renal injury recovery, and facilitating wound healing [9]. Besides, exosomes, nanosized extracellular vesicles function as carriers because of their composition of lipid bilayer, proteins and RNAs, and exosomes released by MSCs alleviate ischemia/reperfusion (I/R)-induced renal injury [10]. The hucMSCs derived exosomes (hucMSC-exo) reduce hepatic inflammation and collagen deposition, accelerate the recovery of hepatocyte

CONTACT Zhigang You youzhigan051303@163.com
© 2020 Informa UK Limited, trading as Taylor & Francis Group

damage, restore liver function and improve liver fibrosis [11]. It has proved that microRNAs (miRs) in MSC-secreted exosomes have curative effects on inflammatory diseases, like sepsis, spinal cord injury and AMI [12]. Among the superfamily, miR-19a prevents hypoxia/reoxygenation (H/R)-induced cardiomyocyte apoptosis and alleviates myocardial ischemic injury with the involvement of protein kinase B (AKT) pathway [13]. In this study, we found miR-19a could target SOX6. As is recently reported, miR-499-5p inhibits H/R-induced cardiomyocytes injury by targeting SOX6 [14]. Besides, the AKT/Jun N-terminal kinase3 (JNK3)/caspase-3 axis is involved in the protection of cerebral I/R injury [15]. Surprisingly, it is recently reported that hucMSC-exo exhibits protective effects on AMI *in vivo* and on cardiomyocyte hypoxia injury *in vitro* via miR-125b-5p and Smad7 [16]. Based on the above references, we hypothesize that there may be potential mechanism of hucMSC-exo in AMI via the regulation of miR-19a, SOX6 and the AKT/JNK3/caspase-3 axis.

2. Materials and methods

2.1. Ethics statement

This study was performed with the approval of the Clinical Ethical Committee of The Second Affiliated Hospital of Nanchang University. Significant efforts were made to minimize the number of animals and their suffering.

2.2. Isolation and identification of hucMSCs

Fresh human umbilical cord tissues (provided by Affiliated Hospital of Jiangsu University, Zhenjiang, Jiangsu, China) were immersed in the culture medium containing penicillin, streptomycin and phosphate buffer saline (PBS) for 20 min, and then sliced into 1 ~ 3 mm^3 sections, followed by cultivation in low glucose-Dulbecco's Modified Eagle's Medium (L-DMEM, Gibco Company, Grand Island, NY, USA) with 10% fetal bovine serum (FBS) at 37°C in a 5% CO_2 incubator for 20 min. When cells appeared around the tissue sections and cell confluence reached 80%, cells were detached with trypsin and passaged until cell fusion. At that time, the hucMSCs were obtained.

The hucMSCs of the third passage were obtained, and the expression of cell surface markers CD105, CD29, CD44 and CD34 was detected using flow cytometer (Beckman Coulter, Inc., Chaska, MN, USA). Adipocyte induction medium and osteoblast induction medium (Gibco Grand Island, NY, USA) were used to induce hucMSCs to differentiate into adipocytes and osteoblasts, respectively. Oil red O staining and alizarin red staining were used to observe the adipogenesis and osteogenesis.

2.3. Isolation and identification of hucMSCs-exo

When hucMSC confluence reached 60% nearly, hucMSCs were continuously cultured for 48 h in FBS-prepared L-DMEM without exosomes. After that, the supernatant was collected and then centrifuged at 20,000 rpm/minute and 4°C for 30 min. Next, the supernatant was moved to the ultrafiltration tube, centrifuged at 50,000 rpm and 4°C for 30 min. The lower concentrated fluid was collected and centrifuged repeatedly until the supernatant was completely concentrated. The concentrated fluid was filtered with a small filter of 0.22 μm and transferred to the ultra-centrifugal tube, centrifuged at 50,000 rpm and 4°C for 1 h. The white precipitation could be seen at the bottom of the tube after centrifugation. Afterward, the supernatant was discarded and the precipitation was suspended by PBS and centrifuged at 3000 rpm/minute at 4°C for 10 min. Finally, the supernatant was purified hucMSC-exo.

The morphology of exosomes was observed under the transmission electron microscope (TEM) (Olympus, Tokyo, Japan). After being dispersed and mixed, 10 μL exosomes were absorbed and stained in 2% phosphotungstic acid negative staining. The size distribution of exosome samples was observed by nanoparticle tracking analysis (NTA). Double-distilled water was added to the measuring tube to the maximum scale. The size and distribution of hucMSC-exo were measured by Nanosight NTA, and analyzed with the Zetasizer-Nano software (Hangzhou Neoline Technology Co., Ltd., Hangzhou, Zhejiang, China). If there were no impurities in double distilled water, 10 μL samples were drawn into the measuring tube and mixed repeatedly. The expression of CD9, CD63, Alix 3 and Cis-Golgi matrix 130 (GM130) on the exosome surface

was detected by western blot analysis and analyzed with Zetasizer-Nano software.

In addition, hucMSCs were seeded in six-well plates at 1×10^4 cells/well 1 day prior to the transfection. On the next day, 5 μL Lipofectamine 2000 (Invitrogen, Carlsbad, CA, USA) was diluted with 125 μL serum-free medium. Then 10 μL of miR-19a mimic, miR-19a inhibitor and negative control (NC) vectors (Shanghai Genechem Co., Ltd., Shanghai, China) were diluted with 125 μL serum-free medium. The above diluted media were mixed and added into the six-well plates (the final concentration of transfected vectors was 100 nmol/L). After 24 h of transfection, the exosomes of each group were extracted according to the above steps, named as in-NC/hucMSC-exo, in-miR-19a/hucMSC-exo, NC/hucMSC-exo and miR-19a/hucMSC-exo, respectively, which were used for subsequent experiments.

2.4. AMI model establishment and grouping

A total of 105 male Sprague Dawley rats (300 ~ 350 g) were provided by Chongqing Medical University (Chongqing, China, Certified No: SYXK (Yu) 2017–0012). The rats were raised in a specific pathogen-free grade room at 25°C with 50% ~ 80% humidity, and rats had free access to feed and water. Fifteen rats were allocated into the sham group and the remaining rats were used for AMI modeling. The rats were anesthetized, endotracheal intubation was performed for mechanical ventilation and electrocardiograph (EGG) changes were closely monitored. After thoracotomy, the proximal segment of the anterior descending branch of the left coronary artery was identified and ligated. If the myocardial color became darker, the heart enlarged, the regional myocardial motion of left ventricular anterior wall weakened obviously, and the ST segment of EGG elevated after ligation of coronary artery, the AMI model was established successfully. After judgment, the thoracic incision of rats was sutured and rats were put back into cages. As for rats in the sham group, the anterior descending branch of left coronary artery was not ligated, and the other steps were the same as those in AMI rats.

Rats were allocated into AMI + PBS group (AMI rats were injected with equal amount of PBS), AMI + hucMSC-exo group (AMI rats were injected with 400 μg/g hucMSC-exo), AMI + in-NC/hucMSC-exo group (AMI rats were injected with 400 μg/g in-NC /hucMSC-exo), AMI + in-miR-19a/hucMSC-exo group (AMI rats were injected with 400 μg/g in-miR -19a/hucMSC-exo), AMI + NC/hucMSC-exo group (AMI rats were injected with 400 μg/g NC/hucMSC-exo), and AMI + miR-19a/hucMSC-exo group (AMI rats were injected with 400 μg/g miR-19a/hucMSC-exo), with 15 rats in each group. All rats were used for echocardiograph detection and serum detection. After blood collection, myocardial tissue homogenate was prepared from five rats for reverse transcription quantitative polymerase chain reaction (RT-qPCR), five rats for 2,3,5-Triphenyltetrazolium chloride (TTC) staining, and five rats for hematoxylin and eosin (HE) staining and terminal deoxynucleotidyl transferase (TdT)-mediated dUTP nick end labeling (TUNEL) assay.

2.5. RT-qPCR

Total RNA from hucMSCs and tissue homogenate was obtained using the Trizol (Invitrogen) to determine its concentration and purity, and then reversely transcribed into cDNA. The mRNA expression was quantified by SYBR PCR Master Mix kit (Applied Biosystems, Inc., Carlsbad, CA, USA) with U6 as a reference for miR-19a and β-actin for SOX6. The primers used in the experiment were designed by Primer 3Plus website and synthesized by Suzhou Genewiz Bio-engineering Co., Ltd (Suzhou, Jiangsu, China). The experiment was repeated for three times. The primers are shown in Table 1.

2.6. Echocardiograph detection

Rats in each group were anesthetized with 1% pentobarbital sodium solution and taken supine position. Left ventricular end systolic diameter (LVESD) and left ventricular end diastolic diameter (LVEDD) were measured by Vevo 2100. Left ventricular ejection fraction (LVEF) and left ventricular fractional shortening (LVFS) were computed automatically by echocardiographic computer. The mean values of six-consecutive cardiac cycles were obtained.

Table 1. Primer sequence for RT-qPCR.

Primer	Sequence (5′→3′)
miR-19a	F: CAATCCTCTCAGGCTCAGTCC
miR-19a	R: TATGCTTGTTCTCGTCTCTGTGTC
U6	F: CTCGCTTCGGCAGCACA
U6	R: GTGTCGTGGAGTCGGCAA
SOX6	F: CCCCTCTGAACATGGTGGTGGC
SOX6	R: TGAGAC TGCCCCTGCCGAGT
β-actin	F: GTCATTCCAAATATGAGAGATGCGT
β-actin	R: GCTATCACCTCCCCTGTGTG

Note: F, forward; R, reverse; miR-19a, microRNA-19a; RT-qPCR, reverse transcription quantitative polymerase chain reaction.

2.7. Enzyme-linked immunosorbent assay (ELISA)

After ultrasonography, 1 mL orbital blood was collected, stood at room temperature for 30 min, centrifuged at 3500 rpm and 4°C to separate serum. According to the detection kits of interleukin (IL)-1β and IL-18 (Shanghai Bohu Biotechnology Co., Ltd., Shanghai, China), cardiac troponin T (cTnT), creatine kinase isoenzyme MB (CK-MB) and lactate dehydrogenase (LDH) kits (BIOSINO Technology&Science Co., Ltd., Beijing, China), the levels of serum myocardial injury markers and inflammatory factors were measured. The serum levels of IL-1β, IL-18, cTnT, CK-MB and LDH were then determined by double-antibody sandwich ELISA.

2.8. HE staining

After blood collection, 3% pentobarbital sodium was injected into the abdominal cavity, and the heart was cut into six pieces after thoracotomy, and fixed in 10% neutral formalin solution for 48 h. After alcohol gradient dehydration, xylene soaking, wax immersion and embedding, the waxed blocks were fixed on the slicing machine and sliced at 3 μm. Tissue sections were stained with hematoxylin, washed in water, and differentiated with 75% ethanol hydrochloride. Afterward, the sections were washed in water and stained with eosin for 12 min. Next, sections were washed, dehydrated, cleaned and sealed. The morphology of cardiomyocytes was observed under an ordinary optical microscope.

2.9. TUNEL assay

Myocardial sections of rats in each group were taken for detecting myocardial apoptotic index using TUNEL method as per the instructions of the kit (Boster Biological Technology Co., Ltd, Wuhan, Hubei, China). Diaminobenzidine (0.3 mL/L) color solution was used for color development, and sections were counterstained with hematoxylin for 30 s, cleaned with xylene and sealed with neutral gum after dehydration with gradient alcohol. Finally, sections were photographed under the microscope. The cells stained brown and yellow were positive cells. The apoptotic rate = the number of positive cells/total nuclei × 100%.

2.10. TTC staining

Rats in each group after blood collection were injected with 1 mL Evans blue (0.1 g/mL) via the tail vein. After 1 min, the hearts of the rats were removed immediately after thoracotomy and stored at −20°C for 20 min. Four to five sections were cut at 1.0 to 1.5 mm along the vertical axis. Each section was pressed with slides and stained with 1% TTC dyeing (NanJing JianCheng Bioengineering Institute, Nanjing, Jiangsu, China) at 37°C for 30 min, and then fixed with 4% polyformaldehyde solution. The infarcted heart was white and the non-infarcted heart was red. The images were acquired by a digital camera, and the infarct size = infarct size/(infarct size + non-infarct size) × 100%, which was calculated by Image J software.

2.11. Establishment and grouping of hypoxic cell model

H9C2 cells (Cell Bank of Shanghai Institutes of Biological Sciences, Chinese Academy of Sciences, Shanghai, China) were inoculated into 96-well plates at 1.5×10^4 cells/well, and 1200 μmol/L $CoCl_2$ (Sigma-Aldrich, Merck KGaA, Darmstadt, Germany) was added into the culture medium for 24 h to establish a cell model of myocardial hypoxia. H9C2 cells were assigned into eight groups, namely the control group (H9C2 cells were treated with normoxia + PBS), Hypoxia group (hypoxic H9C2 cells were treated with PBS), Hypoxia + hucMSC-exo group (hypoxic H9C2 cells were treated hucMSC-exo), Hypoxia + in-NC/hucMSC-exo group (hypoxic H9C2 cells were treated with hucMSC-exo + miR-19a inhibitor NC), Hypoxia + in-miR-19a/hucMSC-exo group (hypoxic H9C2 cells were treated with hucMSC-exo + miR-19a

inhibitor), and Hypoxia + in-miR-19a/hucMSC-exo + si-SOX6 group (hypoxic H9C2 cells were treated with hucMSC-exo + miR-19a inhibitor + si-SOX6), Hypoxia + NC/hucMSC-exo group (hypoxic H9C2 cells were treated with hucMSC-exo + miR-19a NC) and Hypoxia + miR-19a/hucMSC-exo group (hypoxic H9C2 cells were treated with hucMSC-exo + miR-19a NC).

H9C2 cells were seeded in six-well plates at 5×10^4 cells/well 1 day prior to the transfection. On the next day, 5 μL Lipofectamine 2000 was diluted with 125 μL serum-free medium. Then 10 μL of si-SOX6 (Shanghai Genechem) were diluted with 125 μL serum-free medium. The above diluted media were mixed and added into the six-well plates (the final concentration of si-SOX6 was 100 nmol/L). After 24 h of transfection, subsequent experiments were carried out.

2.12. 3-(4, 5-dimethylthiazol-2-yl)-2, 5-diphenyltetrazolium bromide (MTT) assay

Each well was added with 20 μL MTT solution (5 mg/mL) and cultured for 4 h avoiding exposure to light. Next, the culture medium was removed, and cells were added with 150 μL dimethyl sulfoxide (DMSO) solution, vibrating for 10 min to fully dissolve the crystals. Absorbance (A) value was determined at 570 nm by a microplate reader. A blank group was set, in which the corresponding amount of culture medium and MTT solution were added, but without DMSO solution. Six duplicated wells were set in each group, and the experiment was repeated three times. Cell survival rate = (A1-A0)/(A2-A0), in which A1 was the absorbance of the Hypoxia group, A2 was the absorbance of the control group, while A0 was the absorbance of the blank group.

2.13. 4′, 6-diamidino-2-phenylindole (DAPI) staining

The culture medium of 24-well plates was discarded and cells in each well were fixed with 4% paraformaldehyde (200 μL) for 10 min. Next, paraformaldehyde was removed and each well was supplemented with 50 μL DAPI solution (Shanghai LMAI Bioengineering Co., Ltd., Shanghai, China). DAPI was discarded when staining for 5 min, and cells were washed with PBS and photographed under an inverted fluorescence microscope to observe the nucleus pyknosis, fusion and rupture.

2.14. Reactive oxygen species (ROS) measurement

Cell culture medium in each group was absorbed and cells were added with 1 mL serum-free medium, and 1 μL Rosup (100 mmol/L) was added into the positive control wells, followed by incubation at 37°C for 1 h in light-shielded condition. One nanoliter probe dichloro-dihydro-fluorescein diacetate (DCFH-DA, 10 mmol/L, MedChemExpress Co., Ltd (Monmouth Junction, New Jersey, USA) was added into the control group and the Hypoxia group, and incubated at 37°C for 30 min in light-shielded condition. Finally, green fluorescence intensity was observed under the inverted fluorescence microscope.

2.15. Detection of LDH release

The release of LDH in each group was detected with LDH kit (Beyotime, Beijing, China) according to the instructions. Spectra Max M5e Multi-Mode Microplate Reader (Molecular Devices, San Jose, CA, USA) was used to detect the absorbance.

2.16. Western blot analysis

Cells in each group were lysed with radioimmunoprecipitation assay lysate to extract proteins. Then the supernatant was absorbed to quantify the proteins. Next, the extra supernatant was moved to a 1.5 mL centrifuged tube, added with corresponding volume of 5 × loading buffer, and then boiled for 10 min. The proteins were run on polyacrylamide gel electrophoresis, and transferred to membranes at 90 mA. After that, the membranes were sealed with 50 g/L milk for 1 h, and incubated with primary antibodies overnight. On the next day, the membranes were incubated with horseradish peroxidase-labeled secondary antibody rabbit anti-mouse immunoglobulin G (IgG, ab6728, 1:2000) and visualized with enhanced chemiluminescence reagent. Bio-Rad Digital Image System (Bio-Rad Laboratories, Inc. Hercules, CA, USA) was applied to analyze the results. The antibodies used are shown in Table 2. All antibodies were purchased from Abcam Inc. (Cambridge, MA, USA).

Table 2. Antibodies used in western blot analysis.

Antibody	Item No.	Dilution ratio
GM130	ab52649	1: 1000
CD9	ab92726	1: 2000
CD63	ab217345	1: 1000
Alix3	ab117600	1: 1000
Bcl-2	ab32124	1: 1000
Bax	ab32503	1: 1000
Cleaved Caspase-3	ab211631	1: 1000
SOX6	ab64946	1: 500
AKT	ab179463	1: 2000
p-AKT	ab38449	1: 1000
JNK3	ab179461	1: 1000
P-JNK3	ab124956	1: 1000
Caspase-3	ab197202	1: 500
β-actin	ab64946	1: 1000
IgG	ab6728	1: 2000

Note: GM130, Golgi matrix 130; Bcl-2, B-cell lymphoma-2; Bax, Bcl-2-associated X; AKT, protein kinase B; JNK3, Jun N-terminal kinase3; IgG, immunoglobulin G.

2.17. Co-culture of exosomes and H9C2 cells

After hypoxic culture of H9C2 cells for 4 h, PKH67 staining reagent (Sigma-Aldrich) was mixed with the extracted exosomes for 3 min, and the exosomes-free FBS was used to terminate the incubation. The stained exosomes were transferred to the ultrafiltration tube (Millipore Corp, Billerica, MA, USA) and washed 3 times. The stained exosomes (PKH67 huMSC-exos) were co-cultured with normal H9C2 cells, and the non-fluorescent exosomes were added to H9C2 cells as a NC (unlabeled huMSC-exo). The co-cultured H9C2 cells were observed under the confocal laser microscope (Olympus, Tokyo, Japan).

2.18. Transwell assay

After 48-h culture, cells were detached with trypsin and suspended in serum-free Roswell Park Memorial Institute-1640 medium. The cells were counted and adjusted to 3×10^5 cells/mL. The apical chamber was covered with 200 μL cells, and basolateral chamber was paved with 600 μL medium containing 20% serum. After 24-h incubation, the chamber was taken out, cell medium in the apical chamber was absorbed, and cells were wiped off with cotton swabs. After PBS washing, cells were fixed with 4% paraformaldehyde for 10 min, then washed once with PBS, and stained with crystal violet stain for 8 min. Following 3 PBS washes, cells were observed, photographed and counted under the microscope (Olympus, Tokyo, Japan) after drying.

2.19. Flow cytometry

After hypoxia and reoxygenation, the cell detachment was terminated by adding serum-containing culture solution. Cells were collected and centrifuged at 1200 rpm/minute for 8 min with the supernatant discarded. After that, cells were stained with propidium iodide-AnnexinV according to the kit. The apoptotic rate of cardiomyocytes was detected by flow cytometry.

2.20. Dual luciferase reporter gene assay

The SOX6 3'untranslated region (3'UTR) sequence containing the binding site of miR-19a was synthesized, and the wild type (WT) plasmid (SOX6-WT) and mutant type (MUT) plasmid (SOX6-MUT) of SOX6 3'UTR were constructed. The constructed plasmids were mixed with NC and miR-19a plasmids, respectively, and then transfected into HEK293 cells (American Type Culture Collection, ATCC, Manassas, Virginia, USA). Afterward, cells were collected and lysed after transfection for 48 h. Luciferase activity was detected by Luciferase Detection Kit (BioVision, San Francisco, CA, USA) and Glomax 20/20 luminometer (Promega, Madison, Wisconsin, USA).

2.21. Statistical analysis

SPSS 21.0 (IBM Corp., Armonk, NY, USA) was applied for data analysis. Kolmogorov-Smirnov test showed whether the data were in normal distribution. The results were expressed as mean ± standard deviation. Comparison between the two groups was analyzed by *t* test, comparison among multiple groups was analyzed by one-way analysis of variance (ANOVA) or two-way ANOVA, and pairwise comparison after ANOVA was conducted by Sidak's multiple comparisons test or Tukey's multiple comparisons test, respectively. p was obtained by two-tailed test and $p < 0.05$ indicated significant difference.

3. Results

3.1. Identification of hucmsc and hucMSC-exo

The neurites of primary cultured hucMSCs showed fibrous morphology and fingerprint-like or whirlpool-like growth (Figure 1a). *In vitro* specific

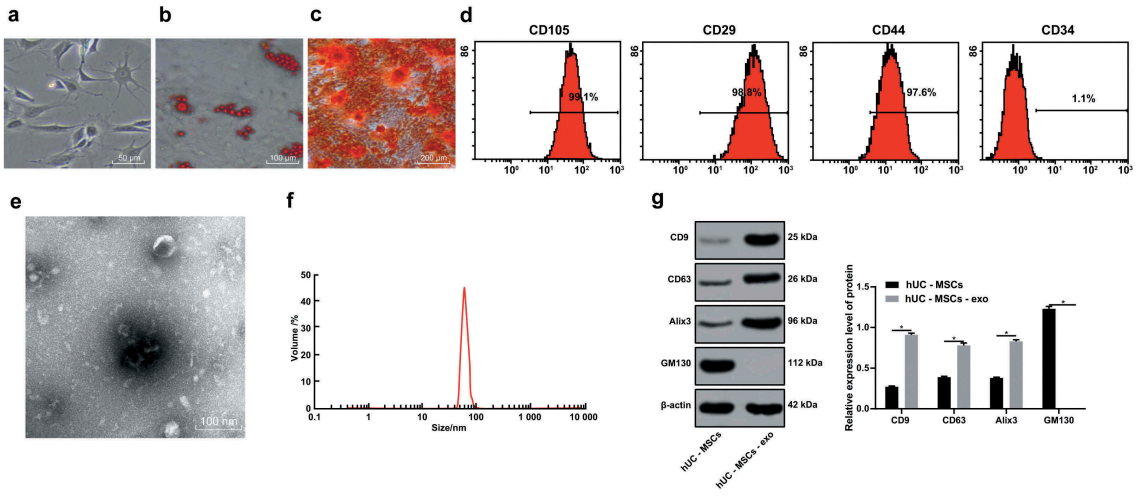

Figure 1. hucMSCs and hucMSC-exo are successfully obtained. (a). Morphology of primary hucMSCs; (b). Cell adipogenesis was induced and red lipid droplets were observed by oil red O staining; (c). A large number of rosy-red calcium nodules were observed during osteogenesis induction by alizarin red staining; (d). Flow cytometry detected the expression of cell surface markers; (e). Morphology of extracted hucMSC-exo observed by TEM; (f). Nanosight NTA measured particle size distribution of hucMSC-exo; (g). Western blot analysis measured hucMSC-exo surface markers GM130, CD9, CD63 and Alix3. For pairwise comparisons, * $p < 0.05$. The experiment was repeated for three times. Data in panel G were analyzed by two-way ANOVA, and Sidak's multiple comparisons test was used for pairwise comparison after ANOVA. hucMSCs, human umbilical cord mesenchymal stem cells; hucMSC-exo, human umbilical cord mesenchymal stem cells-exosomes; TEM, transmission electron microscope; NTA, nanoparticle tracking analyzer; GM130, Golgi matrix 130; ANOVA, analysis of variance.

adipogenic and osteogenic differentiation of the obtained cells showed that cells contained fat particles and were stained red, while the calcium deposits in the cells were stained red (Figure 1b–c). These results indicated that the cultured cells had the characteristics of multidirectional differentiation of MSCs. Flow cytometry was used to detect the expression of cell surface markers. The results exhibited that the cell surface antigen CD34 was negative, while CD105, CD29 and CD44 were positive, meeting the international criteria for MSCs (Figure 1d). In conclusion, hucMSCs were successfully isolated and cultured.

TEM revealed that the exosomes were round or quasi-circular, lipid-coated tea saucer-like microvesicles with a diameter between 30 and 100 nm (Figure 1e). NTA results showed that the size of exosome vesicles varied, and the peak size distribution was at 80 nm, ranging from 40 to 100 nm (figure 1f). Western blot analysis found that exosome surface marker proteins CD9, CD63 and Alix3 were overexpressed, but GM130 was not expressed (Figure 1g), indicating the successful extraction of hucMSC-exo.

3.2. HucMSC-exo is protective of AMI in rats

MSCs can differentiate into cardiomyocytes and intravenous injection of MSCs improves cardiac function after AMI [17]. In light of this, we suppose the exosomes in hucMSCs may have the same features. It was found that LVESD and LVEDD were significantly increased and LVEF and LVFS were decreased in AMI rats (all $p < 0.05$, Figure 2a). The levels of IL-1β, IL-18, cTnT, CK-MB and LDH were markedly increased in AMI rats (Figure 2b). The cardiomyocytes arranged in disorder, and infarct size and the apoptotic rate were notably increased (all $p < 0.05$, Figure 2c–e). After injection of exosomes, the indexes showed opposite trends. The cardiomyocytes arranged regularly, fibers were rarely broken, and nucleus morphology tended to be normal. In conclusion, exosomes derived from hucMSC had protective effects on AMI.

3.3. HucMSC-exo attenuates the injury of AMI in rats by releasing miR-19a

Evidences have shown that circulating miRs usually exist in exosomes [18]. RNA in exosomes can shuttle between cells and participate in the regulation of gene expression in receptor cells [19]. It has also been reported that miR-19a/19b can reduce the cardiac damage caused by myocardial infarction and protect cardiac function [20]. Therefore, we speculated that the protective effect of hucMSC-exo on AMI may also

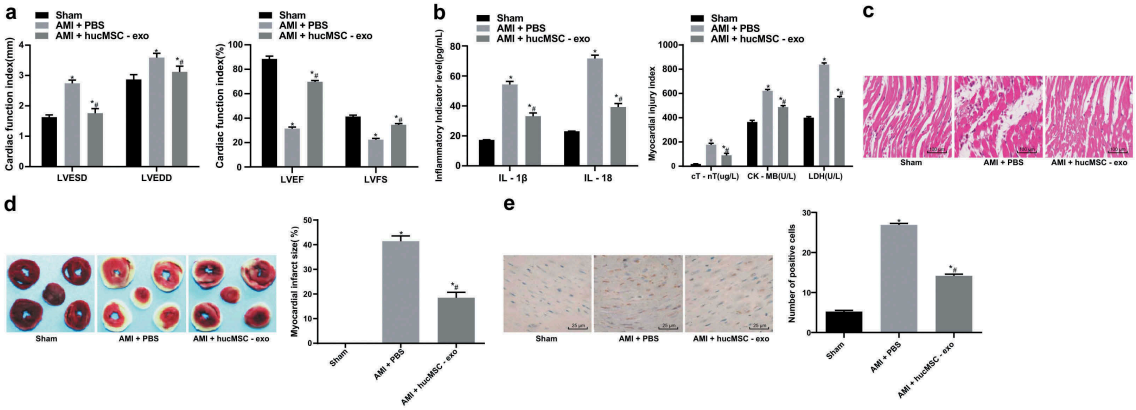

Figure 2. hucMSC-exo is protective of AMI in rats. (a). Cardiac function indexes LVESD, LVEDD, LVEF and LVFS in rats of each group were measured by echocardiography (n = 15); (b). The levels of inflammatory factors IL-1β and IL-18, serum myocardial injury markers cTnT, CK-MB and LDH were measured by ELISA (n = 15); (c). Representative images of histopathological changes of rat hearts detected by HE staining (n = 5); (d). The myocardial infarct size was measured by TTC staining (n = 5); (e). Apoptosis of rat heart tissues detected by TUNEL assay (n = 5). Compared with the sham group, *$p < 0.05$; compared with the AMI + PBS group, # $p < 0.05$. Repetition = 3. Data in panels A and B were analyzed by two-way ANOVA, and Tukey's multiple comparisons test was used for pairwise comparison after ANOVA. Data in panels D and E were analyzed by one-way ANOVA, and Tukey's multiple comparisons test was used for pairwise comparison after ANOVA. hucMSC-exo, human umbilical cord mesenchymal stem cells-exosomes; AMI, acute myocardial infarction; LVESD, left ventricular end systolic diameter; LVEDD, left ventricular end diastolic diameter; LVEF, left ventricular ejection fraction; LVFS, left ventricular fractional shortening; IL, interleukin; cTnT, cardiac troponin T; CK-MB, creatine kinase isoenzyme MB; LDH, lactate dehydrogenase; ELISA, enzyme-linked immunosorbent assay; HE, hematoxylin and eosin; TTC, 2,3,5-Triphenyltetrazolium chloride; TUNEL, terminal deoxynucleotidyl transferase (TdT)-mediated dUTP nick end labeling; ANOVA, analysis of variance.

be related to miR-19a. Observations revealed that miR-19a expression was higher in normal myocardial tissues and cardiomyocytes, but lower in myocardial tissues of AMI rats and hypoxic cardiomyocytes. miR-19a expression was notably increased after hucMSC-exo treatment ($p< 0.05$). After knocking down/overexpressing miR-19a in hucMSCs, miR-19a expression in hucMSC-exo was decreased/increased noticeably (all $p < 0.05$) (Figure 3a). After injecting hucMSC-exo with knockdown/overexpressing miR-19a into rats, it was found that hucMSC-exo with low expression of miR-19a decreased the myocardial protection of AMI rats, while hucMSC-exo with overexpression of miR-19a enhanced the myocardial protection of AMI rats ($p < 0.05$) (Figure 3b-f). In a word, miR-19a knockdown in hucMSC-exo impaired the protective effects of hucMSC-exo on AMI.

3.4. HucMSC-exo alleviates the damage of hypoxic cardiomyocytes

In order to verify whether the exosomes can be absorbed by cells, hucMSC-exos were labeled with PKH67 fluorescent dyeing, and then co-cultured with normal H9C2 cells for 24 h. Under the laser confocal microscope, green fluorescence was observed on the surface of H9C2 cell membrane, but not on the surface of H9C2 cell membrane incubated with unlabeled fluorescent exosomes (Figure 4a). Briefly, hucMSC-exos can be absorbed by normal cells.

Compared with normoxic cells, the nuclear shrinkage rate, LDH and ROS release of H9C2 cells increased significantly under hypoxia (Figure 4b–d), indicating the successful establishment of AMI model. Compared with the hypoxic H9C2 cells, those cultured with hucMSC-exo, in-miR-19a/hucMSC-exo or miR-19a/hucMSC-exo showed increased proliferation and migration, normal nuclear morphology, decreased apoptotic rate, with decreased Cleaved caspase-3 and Bax, and increased Bcl-2 (all $p < 0.05$) (Figure 4e–i). In conclusion, hucMSC-exo inhibited apoptosis and promoted proliferation and migration of hypoxic cardiomyocytes. In addition, we also found that miR-19a/hucMSC-exo had stronger effect on cardiomyocytes than that of in-miR-19a/hucMSC-exo.

3.5. miR-19a targets SOX6

Previously, it has been reported that miR-499-5p inhibits H/R-induced cardiomyocyte injury by

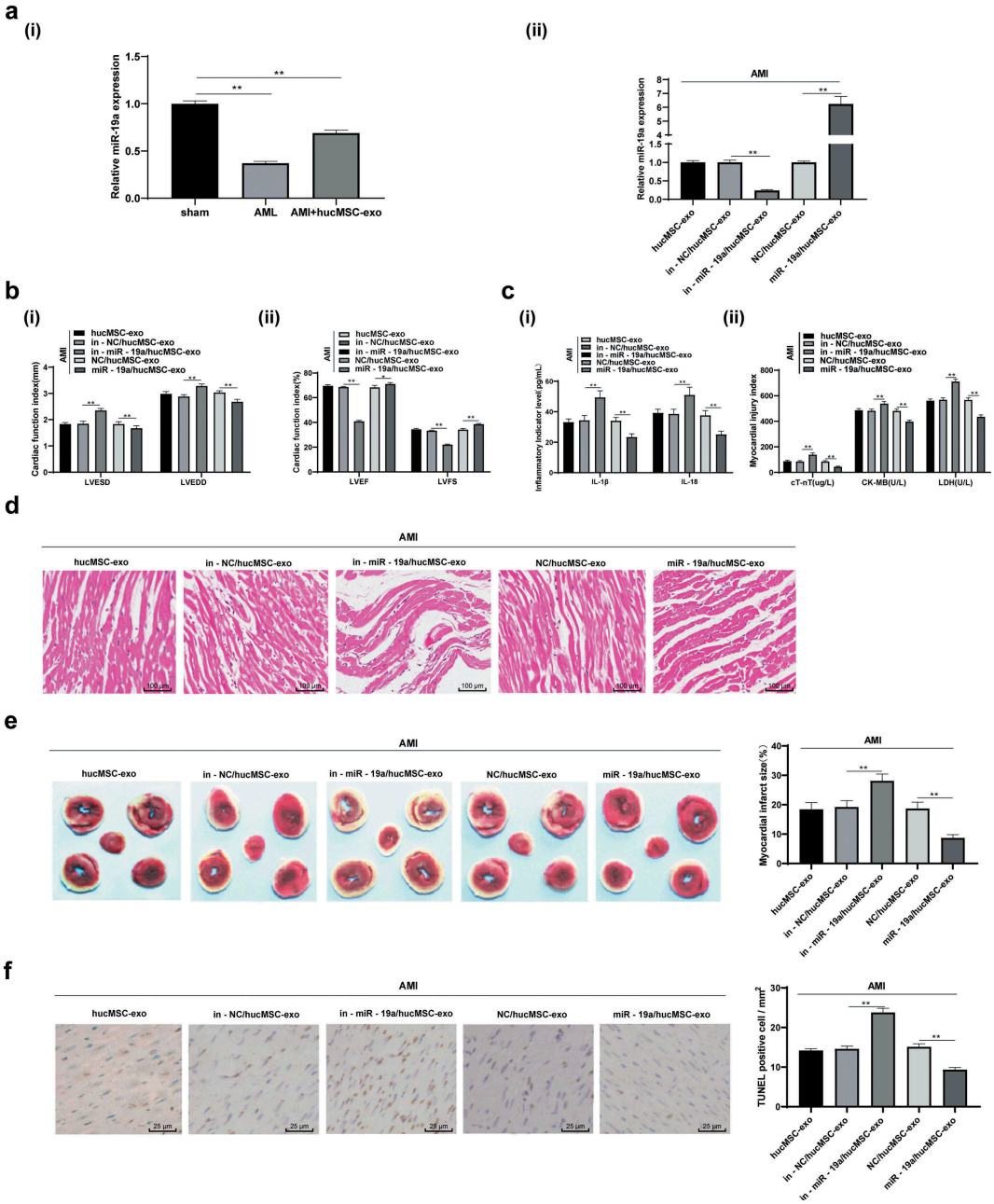

Figure 3. hucMSC-exo attenuates AMI injury in rats by releasing miR-19a. (a). Relative miR-19a expression in AMI tissues measured by RT-qPCR; (b). Relative LVESD, LVEDD, LVEF and LVFS measured by echocardiograph detection, n = 15; (c). Relative levels of IL-1β, IL-18, cT-Nt, CK-MB and LDH measured by ELISA, n = 15; (d). Representative images of histopathological changes of rat hearts detected by HE staining (n = 5); (e). The myocardial infarct size was measured by TTC staining (n = 5); (f). Apoptosis of rat heart tissues detected by TUNEL assay (n = 5). $^{**}p < 0.01$. All experiments were repeated for three times. Data in panel A, E and F were analyzed by one-way ANOVA, and Tukey's multiple comparisons test was used for pairwise comparison after ANOVA. Data in panel B and C were analyzed by two-way ANOVA, and Tukey's multiple comparisons test was used for pairwise comparison after ANOVA. hucMSC-exo, human umbilical cord mesenchymal stem cells-exosome; miR-19a, microRNA-19a; AMI, acute myocardial infarction; RT-qPCR, reverse transcription quantitative polymerase chain reaction; LVESD, left ventricular end systolic diameter; LVEDD, left ventricular end diastolic diameter; LVEF, left ventricular ejection fraction; LVFS, left ventricular fractional shortening; IL, interleukin; cTnT, cardiac troponin T; CK-MB, creatine kinase isoenzyme MB; LDH, lactate dehydrogenase; ELISA, enzyme-linked immunosorbent assay; HE, hematoxylin and eosin; TTC, 2,3,5-Triphenyltetrazolium chloride; TUNEL, terminal deoxynucleotidyl transferase (TdT)-mediated dUTP nick end labeling; ANOVA, analysis of variance.

targeting SOX6 [14]. It encouraged us to figure-out whether miR-19a also reduced cardiomyocyte injury by targeting SOX6. The bioinformatics website www.microrna.org/microrna/getMrna.do?gene predicted that there were binding sites between miR-19a and SOX6 (Figure 5a). Dual luciferase reporter gene

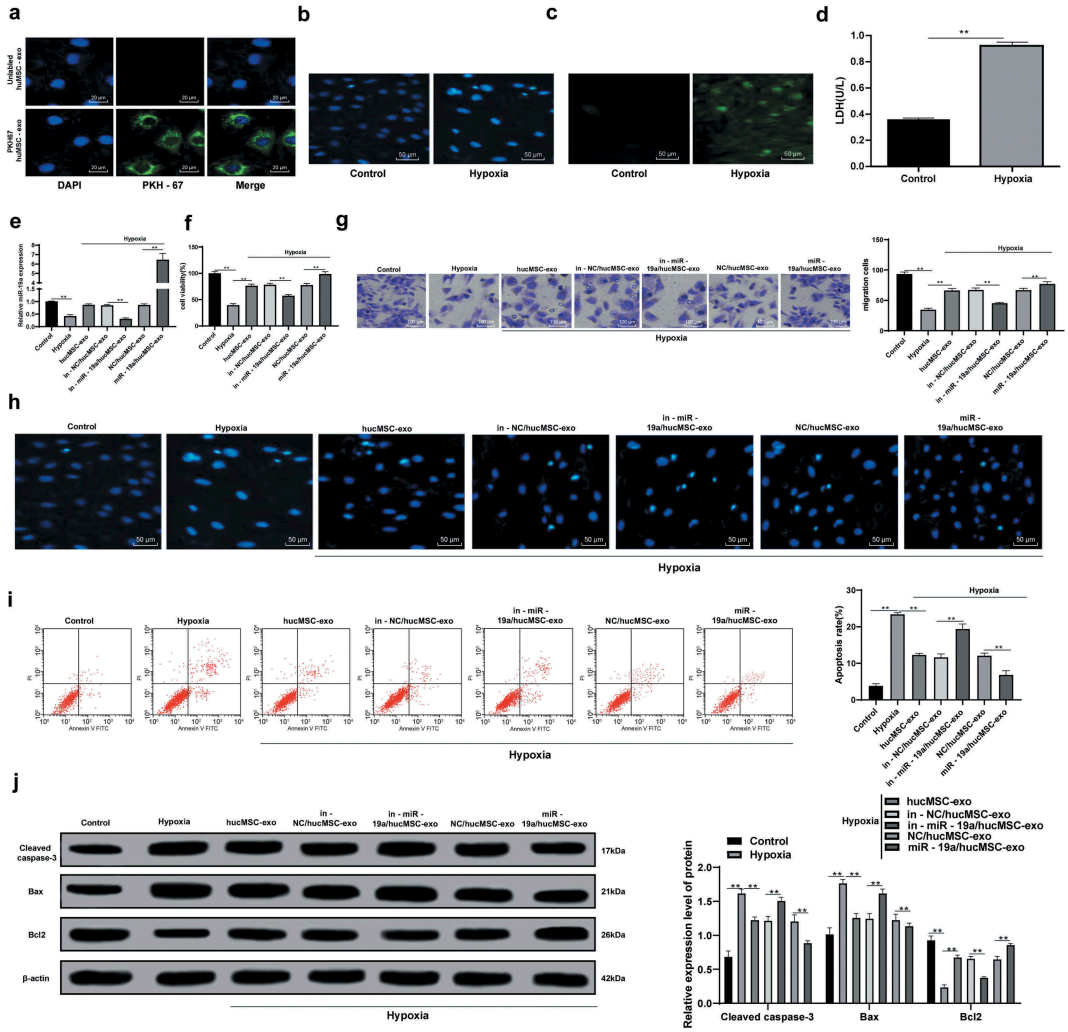

Figure 4. hucMSC-exo with overexpressing miR-19a alleviates the damage of hypoxic cardiomyocytes. (a). Representative images of co-culture of hucMSC-exo and normal H9C2 cells detected by PKH67 staining reagent, and the nuclei were stained with DAPI. The green was PKH67 stained cells and blue was DAPI stained nuclei; (b). Representative images of morphology of normal H9C2 cells and hypoxic H9C2 nuclei detected by DAPI staining; (c). Representative images of ROS accumulation in normal H9C2 cells and hypoxic H9C2 cells detected by DCFH fluorescence; (d). LDH release of normal H9C2 cells and hypoxic H9C2 cells detected by microplate assay; (e). H9C2 cell viability detected by MTT assay; (f). miR-19aexpression in H9C2 cells detected by RT-qPCR; (g). H9C2 cell migration detected by Transwell assay; (h). Representative images of morphology of H9C2 cell nuclei with exosome treatment detected by DAPI staining; (i). Apoptotic rate of H9C2 cells with exosome treatment detected by flow cytometry; (j). Protein levels of Bcl-2, Bax and Cleaved Caspase-3 in H9C2 cells with exosome treatment detected by western blot analysis. $^{**}p < 0.01$. All experiments were repeated for three times. Data in panel D were analyzed by independent *t* test, while data in panel E, F, H and I were analyzed by one-way ANOVA, and Tukey's multiple comparisons test was used for pairwise comparison after ANOVA. Data in panel J were analyzed by two-way ANOVA, and Tukey's multiple comparisons test was used for pairwise comparison after ANOVA. hucMSC-exo, human umbilical cord mesenchymal stem cells-exosome; DAPI, 4′, 6-diamidino-2-phenylindole; DCFH, dichloro-dihydro-fluorescein; LDH, lactate dehydrogenase; ROS, reactive oxygen species; MTT, 3-(4, 5-dimethylthiazol-2-yl)-2, 5-diphenyltetrazolium bromide; Bcl-2, B-cell lymphoma-2; Bax, Bcl-2-associated X; ANOVA, analysis of variance.

assay found the luciferase activity of miR-19a with SOX6-WT was deceased and confirmed the targeting relationship between miR-19a with SOX6 (Figure 5b). Besides, the mRNA and protein levels of SOX6 were remarkably increased in hypoxic H9C2 cells with hucMSC-exo and miR-19a knockdown (both $p < 0.05$, Figure 5c–d), which were apposite when miR-19a was overexpressed.

3.6 Downregulation of SOX6 alleviates AMI damage

Considering SOX6 is a target gene of miR-19a, now we turned to explore the role of SOX6 in AMI. Compared with in-miR-19a/hucMSC-exo treatment, in-miR-19a/hucMSC-exo + si-SOX6 treatment noticeably increased proliferation (Figure 6a)

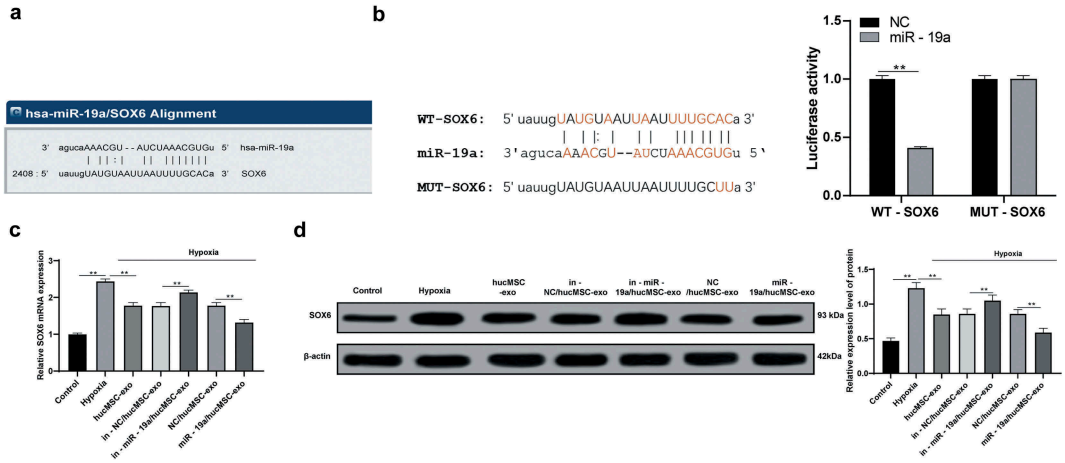

Figure 5. miR-19a could target SOX6. (a). Bioinformatics website predicts the binding sites between miR-19a and SOX6; (b). Dual luciferase reporter gene assay confirmed the targeting relationship between miR-19a with SOX6; (c). Relative SOX6 mRNA expression in hypoxic H9C2 cells with hucMSC-exo or/and miR-19a knockdown measured by RT-qPCR; (d). Relative SOX6 protein level in hypoxic H9C2 cells with hucMSC-exo or/and miR-19a knockdown measured by western blot analysis. $^{**}p < 0.01$. All experiments were repeated for three times. Data in panel B were analyzed by two-way ANOVA, and Sidak's multiple comparisons test was used for pairwise comparison after ANOVA. Data in panels C and D were analyzed by one-way ANOVA, and Tukey's multiple comparisons test was used for pairwise comparison after ANOVA. hucMSC-exo, human umbilical cord mesenchymal stem cells-exosome; miR-19a, microRNA-19a; RT-qPCR, reverse transcription quantitative polymerase chain reaction; ANOVA, analysis of variance.

and migration (Figure 6b) of hypoxic H9C2 cells were, normalized nuclear morphology (Figure 6c), decreased apoptotic rate (Figure 6d) significantly, with decreased Cleaved caspase-3 and Bax, and increased Bcl-2 (all $p < 0.05$) (Figure 6e). Therefore, we concluded that knocking down SOX6 enhanced the protective roles of in-miR-19a/hucMSC-exo against AMI damage.

3.7. HucMSC-exo protects cardiomyocytes by activating AKT and inhibiting JNK3/caspase-3 activation via transferring miR-19a

It has been reported that rosmarinic acid protects hippocampal CA1 neurons from ischemic injury through the AKT/JNK3/caspase-3 axis [15]. AKT/JNK3/caspase-3 is an important mitochondrial apoptotic pathway and has protective effects on cerebral I/R injury in rats [21]. Therefore, we speculate that AKT/JNK3/caspase-3 axis also has an effect on hypoxic damaged cardiomyocytes. After hypoxia treatment, p-AKT decreased significantly, p-JNK3 and caspase-3 increased (all $p < 0.05$), which were reversed by exosome treatment. After overexpressing miR-19a in hucMSC-exo, AKT pathway-related proteins were markedly decreased, while JNK3/caspase-3-related proteins were increased (all $p < 0.05$) (Figure 7).

4. Discussion

The mortality rate of myocardial infarction is still high, despite great efforts have been made to achieve good glucose control and drug treatment [22]. Evidences have shown that stem cell therapy in acute stage of myocardial infarction can prevent apoptosis of cardiomyocytes, facilitate angiogenesis, improve myocardial perfusion and alleviate inflammation [23]. Inspired by this demonstration, we performed a host of experiments to justify the hypothesis and evaluate the potential mechanism of hucMSC-exo in AMI. Collectively, we came to a conclusion that hucMSC-exo protected cardiomyocytes from AMI injury by transferring miR-19a, targeting SOX6, activating AKT, and inhibiting JNK3/caspase-3 activation.

In vivo, hucMSC-exo decreased LVESD and LVEDD, increased LVEF and LVFS, and markedly diminished levels of IL-1β, IL-18, cTnT, CK-MB and LDH in AMI rats, thus playing a protective role in AMI rats. cTnT is of critical importance and believed as the gold standard for detection of acute myocardial necrosis in clinical settings, thus serving as a biomarker for diagnosis and monitoring of myocardial infarction [24]. In AMI patients with ST-segment elevation, increased cTnT was associated with poorer outcomes in spite of early

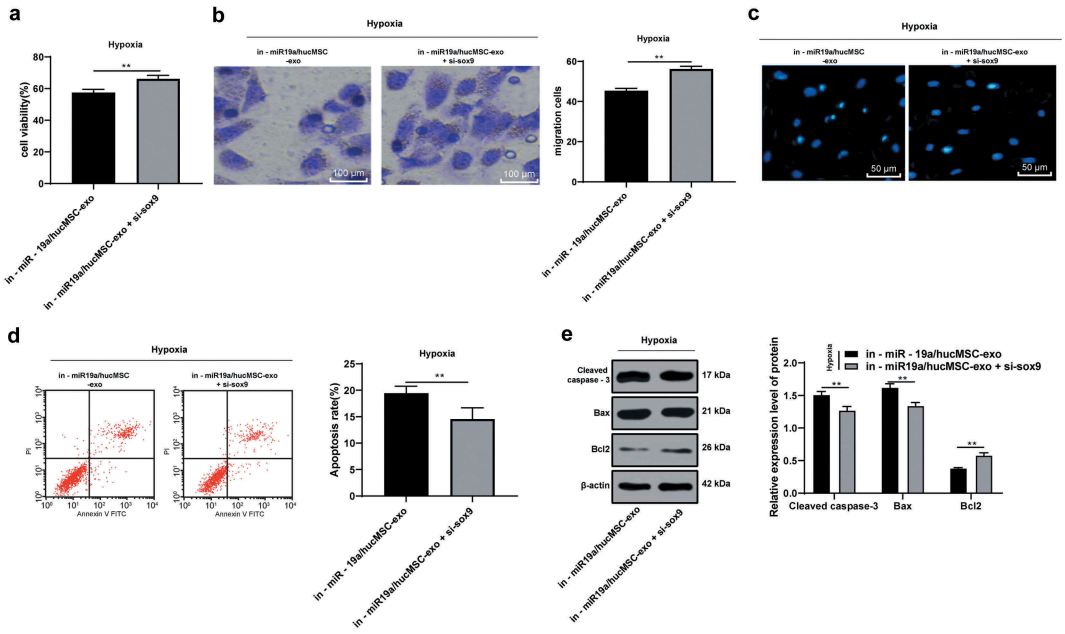

Figure 6. Knocking down SOX6 alleviates AMI damage. (a). H9C2 cell viability in hypoxic H9C2 cells with hucMSC-exo + inhi-miR-19a or/and SOX6 knockdown detected by MTT assay; (b). H9C2 cell migration in hypoxic H9C2 cells with hucMSC-exo + inhi-miR-19a or/and SOX6 knockdown detected by Transwell assay; (c). Representative images of morphology of hypoxic H9C2 cell nuclei with hucMSC-exo + inhi-miR-19a or/and SOX6 knockdown detected by DAPI staining; (d). Apoptotic rate of hypoxic H9C2 cells with hucMSC-exo + inhi-miR-19a or/and SOX6 knockdown detected by flow cytometry; (e). Protein levels of Bcl-2, Bax and Cleaved Caspase-3 in hypoxic H9C2 cells with hucMSC-exo + inhi-miR-19a or/and SOX6 knockdown measured by western blot analysis. $^{**}p < 0.01$. All experiments were repeated for 3 times. Data in panels A, B and D were analyzed by independent t test, and data in panel E were analyzed by two-way ANOVA, and Sidak's multiple comparisons test was used for pairwise comparison after ANOVA. hucMSC-exo, human umbilical cord mesenchymal stem cells-exosome; miR-19a, microRNA-19a; AMI, acute myocardial infarction; MTT, 3-(4, 5-dimethylthiazol-2-yl)-2, 5-diphenyltetrazolium bromide; DAPI, 4′, 6-diamidino-2-phenylindole; RT-qPCR, reverse transcription quantitative polymerase chain reaction; Bcl-2, B-cell lymphoma-2; Bax, Bcl-2-associated X; ANOVA, analysis of variance.

reperfusion [25]. As biochemical markers of myocardial necrosis, CK-MB and cTnT begin to elevate after myocardial injury and reach at the maximum values within 24 h [26]. The myocardial damage in AMI patients can be determined by activity of LDH, CK-MB, cTnT, and higher LDH activity is indicative of greater anaerobic respiration intensity during AMI [27]. Kaliyamurthi Venkatachalam et al. have demonstrated that oxidative stress and I/R could induce IL-18 expression and aggravate inflammation and tissue damage, and verified a direct correlation of increased IL-18 with heart failure, acute coronary syndromes and myocardial dysfunction [28]. Consistently, for patients with severe ischemic heart failure, MSC transplantation can diminish LVESD, improve LVEF, stroke volume and myocardial mass, without side effects [12]. Additionally, in this current study, we also found that after hucMSC-exo treatment, H9C2 cell proliferation and migration increased, apoptotic rate decreased, with decreased Cleaved caspase-3 and Bax, and increased Bcl-2. As previously described, administration of hucMSC-exo noticeably ameliorated cardiac systolic function and reduced cardiac fibrosis *in vivo*, and increased Bcl-2 following exposure to low oxygen and promoted migration of cardiomyocytes, thus relieving AMI injury [23]. Similarly, another study has suggested that adipose MSC-derived exosomes suppressed IL-1β, oxidative stress and cleaved caspase 3, but increased Bcl-2 expression in liver I/R injury [29]. Furthermore, a prior research has demonstrated that transplanting MSCs into ischemic myocardium elevated production of angiogenic factors and reduced apoptosis, thus ameliorating myocardial I/R injury [30]. Li et al. have found that co-transplantation of hucMSCs and huc blood-CD34 (+) cells could improve heart function recovery and diminish collagen deposition and cardiomyocyte apoptosis in infarcted myocardium in a rabbit model of myocardial infarction [31]. In conclusion, hucMSC-exo alleviated AMI damage.

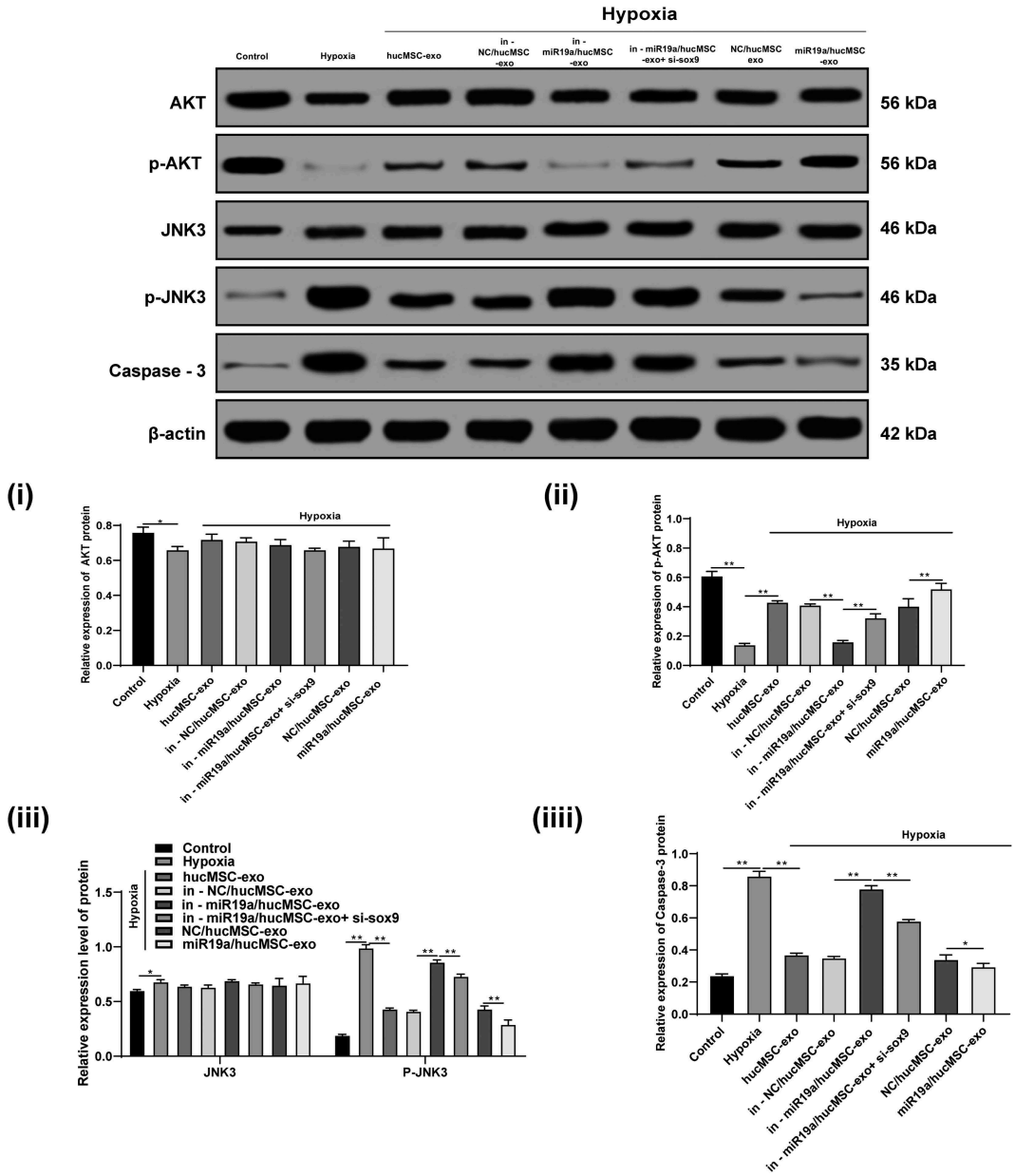

Figure 7. hucMSC-exo-carried miR-19a protects cardiomyocytes by activating AKT and inhibiting JNK3/caspase-3 activation. Protein levels of AKT, JNK 3 and caspase-3 and phosphorylation levels of p-AKT and p-JNK3 were detected by western blot analysis. *$p < 0.05$, **$p < 0.01$. All experiments were repeated for three times. Data in panels i, ii, iv were analyzed by one-way ANOVA and data in panel iii were analyzed by two-way ANOVA, and checked by Tukey's multiple comparisons test for pairwise comparison after ANOVA. hucMSC-exo, human umbilical cord mesenchymal stem cells-exosome; miR-19a, microRNA-19a; AKT, protein kinase B; JNK, Jun N-terminal kinase; ANOVA, analysis of variance.

Furthermore, we observed hucMSC-exo with high miR-19a expression increased H9C2 cell proliferation and migration, while decreased apoptosis. A striking demonstration supported that miR-19a/b family could promote proliferation and survival of ischemic neural progenitor cells and primary cardiomyocytes, and revealed the potential capability of miR-19a/b in cardiac repair and regeneration [32]. Besides, miR-19a-3p was also evaluated to inhibit cardiac hypertrophy, cardiac remodeling and heart failure [33]. Importantly, Gao et al. have stated that overexpression of miR-19a/19b substantially diminished Cleaved caspase3 levels and inflammation, preserved cardiac function and reduced infarct size, thus showing therapeutic roles in cardiac regeneration and protection from myocardial infarction [20]. Additionally, we found miR-19a could target SOX6 and knocking down SOX6 alleviated AMI damage.

Similar to our study, a study has highlighted that SOX6 knockdown rescued cardiac function, maintain the balance of fast- and slow- myofiber gene expression, thus supporting normal heart function [34]. A similar observation noted that miR-499 in cardiac stem cells inhibited its target – SOX6 expression, restored myocardial mass and function in infarcted heart, and enhanced myocardial development after infarction [35]. Moreover, the findings in this present study also indicated that miR-19a in hucMSC-exo protected cardiomyocytes against AMI injury by activating AKT and inhibiting JNK3/caspase-3 activation. It is reported that quercetin improved cerebral I/R-induced cognitive defects by inhibiting apoptosis signal-regulating kinase/JNK3/caspase-3 axis and activating AKT [36]. Another study has suggested that MSC-exo reduced infarct size, decreased oxidative stress, enhanced myocardial viability, and resulted in a long-term preservation of cardiac function and reduced adverse remodeling in H9C2 cardiomyocytes by phosphorylating AKT/GSK3 pathway and inhibiting c-JNK signaling after I/R [37]. Restoration of miR-21 in cardiac progenitor cell-derived exosomes has been found to protect cardiomyocyte from oxidative stress-induced apoptosis [38]. What's more, AKT-modified hucMSC-exo is reported to be effective for AMI treatment by promoting angiogenesis [39].

Taken together, such a conclusion can be draw that the protective effects of hucMSC-exo in cardiomyocytes against AMI injury were achieved by transferring miR-19a, targeting SOX6, activating AKT, and inhibiting JNK3/caspase-3 activation. This study may provide novel insights for the understanding of AMI pathogenesis and treatment. More researches are still needed to further validate our results and to verify the application values in clinic setting.

Disclosure statement

No potential conflict of interest was reported by the authors.

Funding

This work was supported by the Natural Science Foundation of Jiangxi Province [20181BAB205083], Jiangxi Provincial Health and Family Planning Commission of Traditional Chinese Medicine Research Project [2017A064], National Natural Science Foundation of China [81860152].

References

[1] Du H, Hao J, Liu F, et al. Apigenin attenuates acute myocardial infarction of rats via the inhibitions of matrix metalloprotease-9 and inflammatory reactions. Int J Clin Exp Med. 2015;8:8854–8859.
[2] Ibanez B, Fuster V, Macaya C, et al. [Modulation of the beta-adrenergic system during acute myocardial infarction: rationale for a new clinical trial]. Rev Esp Cardiol. 2011;64(Suppl 2):28–33.
[3] Martin-Rendon E, Brunskill S, Doree C, et al. Stem cell treatment for acute myocardial infarction. Cochrane Database Syst Rev. 2008;4:CD006536.
[4] Jamil G, Jamil M, Alkhazraji H, et al. Risk factor assessment of young patients with acute myocardial infarction. Am J Cardiovasc Dis. 2013;3:170–174.
[5] Cabello JB, Burls A, Emparanza JI, et al. Oxygen therapy for acute myocardial infarction. Cochrane Database Syst Rev. 2010;6:CD007160.
[6] Mezzaroma E, Toldo S, Farkas D, et al. The inflammasome promotes adverse cardiac remodeling following acute myocardial infarction in the mouse. Proc Natl Acad Sci U S A. 2011;108:19725–19730.
[7] Castro-Manrreza ME, Montesinos JJ. Immunoregulation by mesenchymal stem cells: biological aspects and clinical applications. J Immunol Res. 2015;2015:394917.
[8] Li CY, Wu XY, Tong JB, et al. Comparative analysis of human mesenchymal stem cells from bone marrow and adipose tissue under xeno-free conditions for cell therapy. Stem Cell Res Ther. 2015;6:55.
[9] Yan Y, Jiang W, Tan Y, et al. hucMSC exosome-derived GPX1 is required for the recovery of hepatic oxidant injury. Mol Ther. 2017;25:465–479.
[10] Shen B, Liu J, Zhang F, et al. CCR2 positive exosome released by mesenchymal stem cells suppresses macrophage functions and alleviates ischemia/reperfusion-induced renal injury. Stem Cells Int. 2016;2016:1240301.
[11] Li T, Yan Y, Wang B, et al. Exosomes derived from human umbilical cord mesenchymal stem cells alleviate liver fibrosis. Stem Cells Dev. 2013;22:845–854.
[12] Chen Y, Zhao Y, Chen W, et al. MicroRNA-133 overexpression promotes the therapeutic efficacy of mesenchymal stem cells on acute myocardial infarction. Stem Cell Res Ther. 2017;8:268.
[13] Sun G, Lu Y, Li Y, et al. miR-19a protects cardiomyocytes from hypoxia/reoxygenation-induced apoptosis via PTEN/PI3K/p-Akt pathway. Biosci Rep. 2017;37:BSR20170899
[14] Shi Y, Han Y, Niu L, et al. MiR-499 inhibited hypoxia/reoxygenation induced cardiomyocytes injury by targeting SOX6. Biotechnol Lett. 2019;41:837–847.
[15] Zhang M, Yan H, Li S, et al. Rosmarinic acid protects rat hippocampal neurons from cerebral ischemia/reperfusion injury via the Akt/JNK3/caspase-3 signaling pathway. Brain Res. 2017;1657:9–15.
[16] Wang XL, Zhao YY, Li S, et al. Exosomes derived from human umbilical cord mesenchymal stem cells improve

myocardial repair via upregulation of Smad7. Int J Mol Med. 2018;41:3063–3072.
[17] Nagaya N, Fujii T, Iwase T, et al. Intravenous administration of mesenchymal stem cells improves cardiac function in rats with acute myocardial infarction through angiogenesis and myogenesis. Am J Physiol Heart Circ Physiol. 2004;287:H2670–6.
[18] Valadi H, Ekstrom K, Bossios A, et al. Exosome-mediated transfer of mRNAs and microRNAs is a novel mechanism of genetic exchange between cells. Nat Cell Biol. 2007;9:654–659.
[19] Chiba M, Kimura M, Asari S. Exosomes secreted from human colorectal cancer cell lines contain mRNAs, microRNAs and natural antisense RNAs, that can transfer into the human hepatoma HepG2 and lung cancer A549 cell lines. Oncol Rep. 2012;28:1551–1558.
[20] Gao F, Kataoka M, Liu N, et al. Therapeutic role of miR-19a/19b in cardiac regeneration and protection from myocardial infarction. Nat Commun. 2019;10:1802.
[21] Ge XH, Zhu GJ, Geng DQ, et al. Metformin protects the brain against ischemia/reperfusion injury through PI3K/Akt1/JNK3 signaling pathways in rats. Physiol Behav. 2017;170:115–123.
[22] Mellbin LG, Malmberg K, Norhammar A, et al. Prognostic implications of glucose-lowering treatment in patients with acute myocardial infarction and diabetes: experiences from an extended follow-up of the diabetes mellitus insulin-glucose infusion in acute myocardial infarction (DIGAMI) 2 study. Diabetologia. 2011;54:1308–1317.
[23] Zhao Y, Sun X, Cao W, et al. Exosomes derived from human umbilical cord mesenchymal stem cells relieve acute myocardial ischemic injury. Stem Cells Int. 2015;2015:761643.
[24] Mirzaii-Dizgah I, Riahi E. Salivary high-sensitivity cardiac troponin T levels in patients with acute myocardial infarction. Oral Dis. 2013;19:180–184.
[25] Rasoul S, Nienhuis MB, Ottervanger JP, et al. Predictors of elevated cardiac troponin T on admission in ST-segment elevation myocardial infarction. Ann Clin Biochem. 2006;43:281–286.
[26] Gu YL, Voors AA, Zijlstra F, et al. Comparison of the temporal release pattern of copeptin with conventional biomarkers in acute myocardial infarction. Clin Res Cardiol. 2011;100:1069–1076.
[27] Gopcevic K, Rovcanin B, Kekic D, et al. Matrix metalloproteinases and membrane damage markers in sera of patients with acute myocardial infarction. Mol Cell Biochem. 2011;350:163–168.
[28] Venkatachalam K, Prabhu SD, Reddy VS, et al. Neutralization of interleukin-18 ameliorates ischemia/reperfusion-induced myocardial injury. J Biol Chem. 2009;284:7853–7865.
[29] Sun CK, Chen CH, Chang CL, et al. Melatonin treatment enhances therapeutic effects of exosomes against acute liver ischemia-reperfusion injury. Am J Transl Res. 2017;9:1543–1560.
[30] Lai RC, Arslan F, Lee MM, et al. Exosome secreted by MSC reduces myocardial ischemia/reperfusion injury. Stem Cell Res. 2010;4:214–222.
[31] Li T, Ma Q, Ning M, et al. Cotransplantation of human umbilical cord-derived mesenchymal stem cells and umbilical cord blood-derived CD34(+) cells in a rabbit model of myocardial infarction. Mol Cell Biochem. 2014;387:91–100.
[32] Song DW, Ryu JY, Kim JO, et al. The miR-19a/b family positively regulates cardiomyocyte hypertrophy by targeting atrogin-1 and MuRF-1. Biochem J. 2014;457:151–162.
[33] Liu K, Hao Q, Wei J, et al. MicroRNA-19a/b-3p protect the heart from hypertension-induced pathological cardiac hypertrophy through PDE5A. J Hypertens. 2018;36:1847–1857.
[34] Ding J, Chen J, Wang Y, et al. Trbp regulates heart function through microRNA-mediated Sox6 repression. Nat Genet. 2015;47:776–783.
[35] Hosoda T, Zheng H, Cabral-da-Silva M, et al. Human cardiac stem cell differentiation is regulated by a mircrine mechanism. Circulation. 2011;123:1287–1296.
[36] Pei B, Yang M, Qi X, et al. Quercetin ameliorates ischemia/reperfusion-induced cognitive deficits by inhibiting ASK1/JNK3/caspase-3 by enhancing the Akt signaling pathway. Biochem Biophys Res Commun. 2016;478:199–205.
[37] Arslan F, Lai RC, Smeets MB, et al. Mesenchymal stem cell-derived exosomes increase ATP levels, decrease oxidative stress and activate PI3K/Akt pathway to enhance myocardial viability and prevent adverse remodeling after myocardial ischemia/reperfusion injury. Stem Cell Res. 2013;10:301–312.
[38] Xiao J, Pan Y, Li XH, et al. Cardiac progenitor cell-derived exosomes prevent cardiomyocytes apoptosis through exosomal miR-21 by targeting PDCD4. Cell Death Dis. 2016;7:e2277.
[39] Ma J, Zhao Y, Sun L, et al. Exosomes derived from Akt-modified human umbilical cord mesenchymal stem cells improve cardiac regeneration and promote angiogenesis via activating platelet-derived growth Factor D. Stem Cells Transl Med. 2017;6:51–59.